

# The voltage-gated potassium channels and their relatives

Gary Yellen

Department of Neurobiology, Harvard Medical School, 220 Longwood Avenue, Boston, Massachusetts 02115, USA

**The voltage-gated potassium channels are the prototypical members of a family of membrane signalling proteins. These protein-based machines have pores that pass millions of ions per second across the membrane with astonishing selectivity, and their gates snap open and shut in milliseconds as they sense changes in voltage or ligand concentration. The architectural modules and functional components of these sophisticated signalling molecules are becoming clear, but some important links remain to be elucidated.**

Electricity plays an unavoidable role in biology. Whenever solutes like phosphate compounds, amino acids, or inorganic ions are transported across membranes, the movement of their charge constitutes an electrical current that produces a voltage difference across the membrane. Beyond managing to keep this accumulation of charge from getting too far out of balance, all living cells have developed the ability to exploit a transmembrane electrical potential as an intermediate in the storage of energy and the synthesis of ATP. However, a specialized class of animal cells—neurons, muscle cells and endocrine cells; known collectively as the ‘excitable cells’—have made the management and production of electrical signals into a high art.

Fast electrical signalling is made possible by the slow and steady homeostatic mechanisms that establish the standard environment and content of animal cells: high  $\text{Na}^+$  concentration ( $[\text{Na}^+]$ ) in the blood and extracellular fluid, and high  $[\text{K}^+]$  (but low  $[\text{Na}^+]$  and  $[\text{Ca}^{2+}]$ ) in the cytoplasm. The plasma membrane separates these two compartments. These gradients are established and maintained by active transporters and pumps, which prepares the way for rapid changes in membrane voltage to be produced by passive transport through ion channels. These pore-forming proteins allow ions to flow only ‘downhill’, as dictated by their electrochemical gradients, but they do it rapidly and selectively. Opening a  $\text{Na}^+$ -selective channel permits  $\text{Na}^+$  to flow down its gradient into a cell, making the intracellular voltage more positive. Opening a  $\text{K}^+$ -selective channel permits  $\text{K}^+$  to flow out of a cell and restores the voltage to a negative value. The dimensions of a typical cell and its membrane allow the voltage to be changed rapidly back and forth many times, with relatively small changes in concentration. This is essentially how all cellular electrical signalling is produced.

The ultimate specialization of electrical signalling is the action potential, a stereotyped, millisecond-long electrical signal that is capable of propagating at rates of metres per second along a nerve fibre. As Hodgkin and Huxley showed<sup>1</sup>, this signal is made possible by a rapid feedback process involving a direct action of voltage on ion channels:  $\text{Na}^+$  channels activated (opened) by positive voltage (constituting the positive feedback process), followed by  $\text{K}^+$  channels activated more slowly by positive voltage (the negative feedback).

## Basic channel architecture

The voltage-gated  $\text{K}^+$  channels are the prototypical voltage-gated channels. At their simplest, they are homotetrameric channels, with each subunit containing a voltage sensor and contributing to the central pore. The standard  $\text{K}^+$  channel subunit contains six transmembrane regions, with both amino and carboxy termini on the intracellular side of the membrane (a tetrameric 6TM architecture; see Box 1). The pore-forming subunits of voltage-gated  $\text{Na}^+$  and

$\text{Ca}^{2+}$  channels contain four non-identical repeats of this motif, strung together on a single polypeptide. There is enormous variety within each of these channel families: voltage-gated  $\text{K}^+$  channels alone are made by at least 22 different genes in mammals, with additional variety produced by alternative splicing and heteromultimerization.

Some close relatives of the voltage-gated  $\text{K}^+$  channels share the tetrameric 6TM architecture but differ in key functional features. These include the sensory channels of the photoreceptors and olfactory neurons, which are non-selective ( $\text{Na}^+$  and  $\text{K}^+$ ) channels that are cyclic-nucleotide-gated (the CNG channels) and insensitive to voltage, and the pacemaker channels found in heart muscle and neurons (the HCN channels) that are controlled by both cyclic nucleotides and voltage.

Each of these signalling proteins performs three main functions. Ion permeation is the central function, and the movement of ions through the pore must be fast and ion-selective. This permeation is then regulated by opening and closing of the pore—a set of conformational changes called gating. Finally, the gating is coupled to a sensing mechanism, which detects transmembrane voltage in the core members of the family, but can also be geared to sense  $\text{Ca}^{2+}$ , cyclic nucleotides, and perhaps other cellular signals. From approximately 40 years of electrophysiology and biophysics, a little over a decade of cloning followed by mutagenesis and physiology on cloned channels, and from a few important crystal structures of some bacterial relatives of these channels, we now have a relatively clear picture of how these functions are accomplished.

## Exquisite selectivity with high throughput

$\text{K}^+$  channels are extremely selective in which ions they allow to pass, yet they allow transport rates close to the aqueous diffusion limit. Selectivity and speed are both crucial for the biological function of the channels. As discussed above, in neurons and other cells, the ion specificity of a channel (for example,  $\text{Na}^+$  or  $\text{K}^+$ ) determines the direction of current flow.  $\text{Na}^+$  and  $\text{Ca}^{2+}$  ions flow inward and thus carry positive charge into the cell—because most voltage-activated channels are activated by positive voltage, this further activates channels and produces regenerative excitation.  $\text{K}^+$  ions flowing outward (or  $\text{Cl}^-$  ions flowing inward) reduce the positive charge inside the cell, and terminate (or prevent) excitation.

High flow rates are essential for producing these voltage changes rapidly. A typical action potential in a mammalian neuron requires millions of ions to flow in a millisecond. To accomplish this without using millions of proteins requires that each one have a very high throughput, while maintaining high selectivity.

What are the energetic and structural requirements for rapid permeation? The reason that ions require assistance to cross lipid

Box 1

The tetrameric 6TM architecture of the K<sup>+</sup> channel family

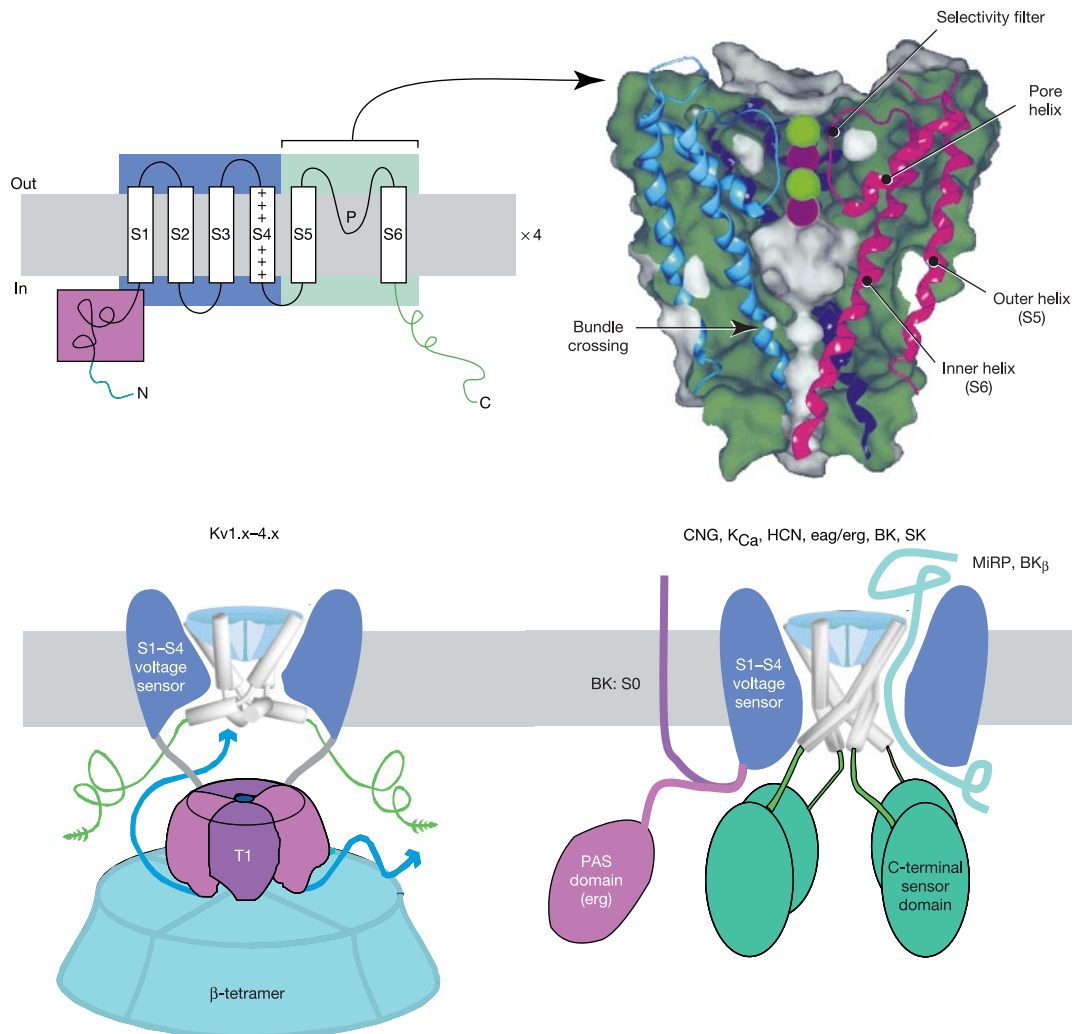
The typical voltage-gated K<sup>+</sup> channel is an assembly of four identical (or similar) transmembrane subunits surrounding a central pore. Each subunit has six transmembrane crossings (S1–S6), with both N- and C termini on the intracellular side of the membrane (top left panel). The narrowest part of the pore, the selectivity filter, is formed by a loop between S5 and S6; the voltage sensor includes the S4 region with its multiple positive charges.

The bacterial KcsA K<sup>+</sup> channel (top right panel, in cross-section) is the prototype for the pore-forming domain of the channel. It has only two transmembrane helices: the outer helix is homologous to S5 and the inner helix to S6. The interior of the protein is dark green, with secondary structure shown as ribbons for three of the four subunits, and the water-exposed surface of the protein is grey. The narrow selectivity filter is seen at the top, with the extended selectivity filter loop supported by the pore helices. The four spheres mark the four K<sup>+</sup> ion binding sites; these are typically occupied by alternating K<sup>+</sup> ions and water molecules<sup>5</sup>. The four inner helices cross to constrict the channel at the bottom (the ‘bundle crossing’). Between the selectivity filter and bundle crossing is the water-filled ‘cavity’.

In the K<sup>+</sup> channel family there are two basic patterns for organizing the structural domains of the channels. All have the central 6TM structure, with a pore domain formed by S5–P–S6 and a voltage sensor comprising S1–S4. The core Kv1.x–Kv4.x subfamily (lower left panel) has at its N terminus a ‘tetramerization domain’ (T1, purple)<sup>3,74</sup> that determines the specificity of subunit assembly<sup>75</sup> and also serves as a

platform for attachment of the optional β-subunits<sup>74</sup> and for other protein–protein interactions. These interactions probably modulate channel activity and may also provide an avenue for the channels to signal directly to intracellular signalling processes<sup>76</sup>. The extreme N terminus can provide the auto-inhibitory ‘ball’ for channel inactivation (see text). The C termini (green) have no obvious domain structure in this subfamily, although there is commonly a PDZ-binding motif<sup>77</sup> that determines the physical localization of the channel and its association into large signalling complexes.

Many other tetrameric 6TM channels have a different domain structure, characterized by the absence of a T1 domain and the presence of a sensor domain in the C terminus (lower right panel). These include the voltage-gated KCNQ and eag/erg channels, as well as channels gated coordinately by voltage and ligand binding (BK Ca<sup>2+</sup>-activated channels and HCN hyperpolarization and nucleotide-gated channels), and channels gated exclusively by intracellular ligands (CNG channels and SK channels). In some cases the C-terminal sensor domains adopt a four-fold symmetrical organization<sup>47</sup>, whereas in other cases they may function as a dimer of dimers<sup>52</sup>. At the N terminus some family members have an additional transmembrane region (S0)<sup>78</sup> or an additional sensor domain<sup>79</sup>. The auxiliary subunits known to be associated with this family (minK, MiRP, BK<sub>β</sub>) are transmembrane; they appear to be intimately associated with the pore domain<sup>80,81</sup> and may displace the voltage-sensor domain or interact with it directly.



membranes is that they have an extremely favourable interaction with water. In the vicinity of a positively charged ion like  $K^+$ , the water molecules re-orient with their negatively charged end towards the ion. In lipid or even in protein, there is no analogous electrostatic accommodation to the presence of the ion (these substances are said to have a relatively low dielectric constant compared with water).

One option for making the  $K^+$  ion stable inside a protein pore would be to use a negative charge. The risk in doing so is that the  $K^+$  ion might become too attracted to the negative charge, and wouldn't exit the pore, as required for a high throughput. This is not the mechanism used by  $K^+$  channels.

Instead, the  $K^+$  channel proteins have four specific architectural features that keep the ion almost exactly as stable as it is in water. First, the channels use plenty of water to make the ion stable. Rather than maintaining a narrow pore of atomic dimension through the entire thickness of the membrane, part of the permeation pathway is broad and contains a large amount of water (see Fig. 1). This explanation was proposed many years ago, particularly as an explanation of the very large conductance of certain  $Ca^{2+}$ -activated  $K^+$  channels<sup>2</sup>, and is borne out in the remarkable crystal structures of the pores of two different bacterial  $K^+$  channels, KcsA and MthK<sup>3–6</sup>.

Second, the  $K^+$  channels apparently stabilize the ions and achieve cation selectivity by using the electrostatic influence of helix dipoles. Every  $\alpha$ -helix has a dipole moment owing to the alignment of the dipoles of its hydrogen bonds, and the intracellular vestibule of  $K^+$  channels has the negative ends of four helix dipoles pointed towards its heart<sup>3</sup>. It has been proposed<sup>3,7</sup> that these helix dipoles produce a preferential stabilization of cations near the entrance to the narrow selectivity filter. This concept is mirrored in the quite different architecture of channels designed to conduct the negatively charged chloride ions—these have the positive ends of multiple helices pointed towards the central ion site<sup>8</sup>.

A third feature of the  $K^+$  channel's approach to permeation and ion selectivity is creation of a series of customized polar oxygen cages. As a  $K^+$  ion diffuses through water itself, it is more or less constantly surrounded by a cage of polar oxygen atoms from the

water molecules. Water is extremely flexible and accommodating, and easily adapts the size and configuration of the cage to accommodate ions of different sizes, such as  $Na^+$  and  $K^+$ . The selectivity filter of the potassium channel is designed to mimic the water structure around a  $K^+$  ion but is also designed not to adopt the presumably more compact structure around a  $Na^+$  ion (as originally proposed by Armstrong<sup>9</sup>). Each  $K^+$  ion in the selectivity filter is surrounded by two groups of four oxygen atoms, just as in water: these oxygen atoms are held in place by the protein, and are in fact the backbone carbonyl oxygens of the selectivity filter loops from the four subunits.

Finally, a long-known feature of potassium channels is that  $K^+$  ions pass through in single file, with simultaneous occupancy by multiple ions<sup>5,10–12</sup>. The mutual electrostatic repulsion between adjacent  $K^+$  ions (spaced about 7 Å apart) destabilizes ions in the pore, permitting the other favourable interactions to produce ion selectivity without producing overly tight binding that would impair rapid permeation.

The structural and architectural features of potassium channels are thus perfectly adapted to fit their function. They solve the electrostatic problem of stabilizing ions—without making them too much more stable than they are in water—by using plenty of water and helix dipoles to counteract the unfavourable dielectric environment within the membrane. Furthermore, they solve the problem of stabilizing potassium in preference to sodium by precisely matching the configuration of oxygen atoms around a solvated potassium ion.

### Gating the pore with conformational motions

To use these transmembrane pores for electrical signalling or even for regulation of ion transport, it is necessary to regulate their permeability. On the slowest timescales, it is possible to control the manufacture of channel proteins by a transcriptional regulatory mechanism; on a more rapid timescale, it is possible to insert multiple channels into the membrane (or withdraw them) by use of a vesicle fusion mechanism. But the very rapid signalling in neurons requires a fast mechanism for closing and opening the pore. There are three established mechanisms by which the voltage-gated  $K^+$  channels can close: two of them involve a conformational constriction of the permeation pathway, and one involves conditional plugging of the pore by an auto-inhibitory part of the channel protein.

### Gating at the S6 bundle crossing

First, the channel can close by pinching shut at the intracellular entrance. This intracellular or S6 gate obstructs entrance from the cytoplasmic surface to the water-filled 'cavity' in the centre of the channel protein. The S6 transmembrane region corresponds to the 'inner helix' of the bacterial KcsA channel. The top (extracellular) ends of the four S6 helices form a cradle for the selectivity filter, whereas the bottom ends converge to a right-handed 'bundle-crossing' below the cavity.

This bundle-crossing corresponds to the functionally determined closure point of at least some of the voltage-gated  $K^+$  channels<sup>13,14</sup>. The S6 transmembrane region and its intracellular extension show very high sequence conservation within the principal families of voltage-gated  $K^+$  channels, and at the bundle crossing there is a strongly conserved proline sequence (PxP or PxG) that is not found in the bacterial  $K^+$  channels. Studies of this region indicate that it is likely to bend the S6 in both the closed and open channels<sup>14–16</sup>.

The probable nature of the S6 opening motion has now been made apparent by the determination of the structure of a second bacterial  $K^+$  channel, MthK<sup>6</sup>, a tetrameric 2TM that can be opened by intracellular  $Ca^{2+}$ . This structure appears to represent the MthK channel in the open state (Fig. 2, centre panel), and it has no bundle crossing: instead, the homologues of the S6 helices are splayed wide open with no constriction between the intracellular solution and the

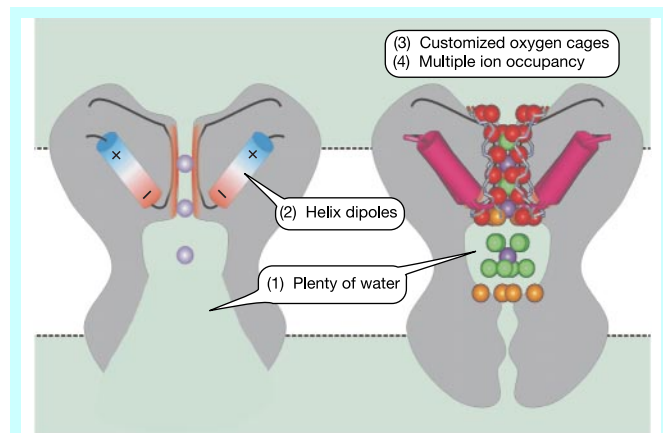


**Figure 1** Architectural features of  $K^+$  channels important for ion permeation. Approximate cross-section of an open  $K^+$  channel, based on the crystal structure of the MthK channel<sup>6</sup> (left). The wide-open intracellular vestibule and pore helix dipoles are highlighted. The diagram on the right is a view derived from the high resolution structure of the KcsA channel<sup>4</sup>, showing a narrower and probably closed access to a water-filled cavity in the middle of the membrane protein. A trapped  $K^+$  ion (purple sphere) and its eight water molecules of hydration (green spheres) are remarkably well resolved; the backbone oxygens of the selectivity filter (red spheres) provide a good match to this hydration environment for the  $K^+$  ions. Occupancy of the pore by multiple  $K^+$  ions has an important role in selectivity and other properties of the channel<sup>5,10–12</sup>. This basic architecture can also produce non-selective cation channels<sup>71</sup> or channels selective for  $Na^+$  or  $Ca^{2+}$  ions<sup>72</sup>. Orange spheres indicate side chain oxygen atoms.

selectivity filter<sup>6</sup>. Comparing this with the presumably closed structure of KcsA gives a plausible picture for the gating motion (Fig. 2, top and centre panels): the S6 helices swing open from an apparent hinge located at a highly conserved glycine residue. The implied motion is much larger than that previously suggested from electron paramagnetic resonance (EPR) measurements on KcsA<sup>17</sup>. It is still unknown whether the voltage-gated channels may use the PxP sequence as a second (or alternative) hinge, or whether the PxP sequence provides a fixed bend that allows the S6 gate of these channels to connect with the transmembrane voltage sensor (rather than to the intracellular calcium sensor used by MthK).

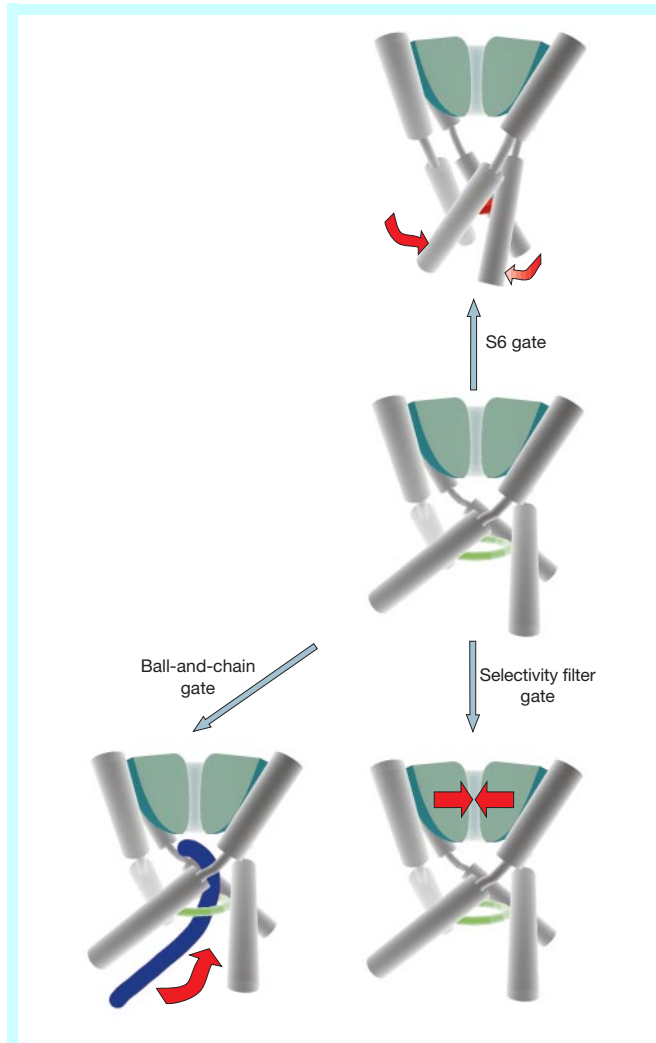


**Figure 2** The conformational changes that gate the K<sup>+</sup> channel pore. The three best-understood conformational changes for closing potassium channels are shown here. The centre diagram shows the core structure of an open K<sup>+</sup>, on the basis of the MthK structure<sup>6</sup>. The selectivity filter (green) is shown with a cutaway to reveal the narrow pore. The outer helices have been stripped away to show the configuration of the inner helices, corresponding to S6. In the open state these are splayed apart, as in the MthK structure, using the conserved glycine hinge near the selectivity filter. The top diagram shows a closed K<sup>+</sup>, on the basis of the KcsA structure<sup>3</sup>. The four S6 transmembrane segments swing together to produce a secure closure at the bundle crossing<sup>14</sup>. This shuts off ion flow and can trap organic channel blockers in the enclosed cavity. The green and red rings in the diagrams illustrate the open and closed states, respectively, of the S6 gates. Alternatively, the channel may be closed at the selectivity filter (lower right diagram), or by binding of an auto-inhibitory peptide (lower left diagram) when a binding site in the pore is revealed by opening of the S6 gate. This figure was prepared with WebLab Viewer (<http://www.accelrys.com>), AC3D (<http://www.ac3d.org>), and POV-Ray (<http://www.povray.org>).

An important consequence of the S6 gating mechanism is its interaction with channel blockers. Small organic blockers, including local anaesthetic-like molecules, act by binding to sites within the cavity. Because of the S6 gate, these blockers can enter the channel only after the channel has been opened (by voltage or another stimulus), and some blockers can be trapped in the cavity when the S6 gate closes<sup>18,19</sup>. The early discovery of these phenomena by Armstrong inspired the initial hypothesis of an intracellular gate<sup>9,18</sup>. Blocker gating and trapping is also a primary mechanism for state-dependent and use-dependent action of channel blockers, a feature that is often crucial to the therapeutic value of channel drugs (for instance, anticonvulsants that must inhibit excessive electrical activity without affecting normal lower levels of activity).

### Ball-and-chain gating

A second mechanism for closing the pore uses the S6 gate to regulate the binding of an auto-inhibitory peptide that is part of the channel protein (Fig. 2, lower right panel). Similar to the small organic blockers studied by Armstrong<sup>9,18</sup>, the N terminus of Shaker K<sup>+</sup> channels can act as a channel blocker, probably by binding directly to the cavity. Because this interaction occurs only after the S6 gate has opened, during the brief period after the S6 gate opens and before the N-terminal peptide blocks the channels: electrophysiologists call this ‘N-type inactivation’.

N-type inactivation (also called the ball-and-chain mechanism because it involves a tethered blocker, initially imagined to be a ball) occurs in several known voltage-gated K<sup>+</sup> channels, and can involve either the N terminus of the principal ( $\alpha$ ) subunit of the channel<sup>20</sup> or the N terminus of an associated  $\beta$ -subunit<sup>21</sup>. It can be disrupted by enzymatic or genetic removal of the N-terminal sequence<sup>20</sup>, and restored by addition of a soluble peptide of the same sequence to the intracellular bathing solution<sup>22</sup>. There is little sequence conservation between the various N termini capable of producing this form of inactivation, although both positive charge and hydrophobic character are important for the interaction with the open channel<sup>23,24</sup>. The peptide appears to inhibit the channel by a simple blocking mechanism: it competes with intracellularly applied channel blockers<sup>25</sup>, is expelled by potassium flow from the opposite side of the membrane<sup>26</sup>, and is specifically affected by mutation of residues within the cavity<sup>27</sup>.

The known form of ball-and-chain inactivation requires an intact S6 gating mechanism, but it is easy to imagine some interesting alternatives. For instance, an S6 gate that could not close all the way might not itself restrict ion movements, but might nevertheless regulate binding of the inhibitory peptide. This would produce a channel that would close whenever the S6 gate is in the open position. Alternatively, instead of using the S6 gate to regulate binding of the peptide, a channel protein might regulate the availability of the N terminus, or limit its access to the inner mouth of the channel. For instance, in one K<sup>+</sup> channel the inactivation process can be eliminated by experimentally induced disulphide formation between the N-terminal ball and another (unidentified) cysteine, effectively tying the ball out of the way<sup>28</sup>. Channel sequences that are antagonistic to ball-and-chain inactivation<sup>29</sup> may function as decoy binding sites, luring the peptide away from its real site of action.  $\beta$ -subunits might regulate the availability of their N-terminal peptide through some action of their as-yet-unknown NAD-dependent enzymatic redox function<sup>30</sup>. Finally, both  $\alpha$ - and  $\beta$ -subunit N termini (as well as permeant ions) must approach the pore through ‘windows’ between the T1 domain and the transmembrane pore domain<sup>31,32</sup> (see Box 1). Access to and through these windows might be restricted by conformational changes or by the binding of protein partners.

### Gating at the selectivity filter

A third mechanism for closing the pore is to pinch shut at the

narrow selectivity filter itself—a selectivity filter or pore gate (Fig. 2, top right panel). This mechanism was first recognized in the form of ‘C-type inactivation’, an alternative to N-type inactivation for producing transient  $K^+$  conductance by closing the channels in spite of a maintained stimulus. C-type inactivation persists in Shaker channels when the inactivation ball is deleted<sup>33</sup>, and it is quite sensitive to extracellular  $[K^+]$  and to mutations at the extracellular entryway to the pore<sup>34</sup>. Closure of this gate can be prevented by the binding of extracellular tetraethylammonium ion (TEA) to the pore<sup>25</sup>; once closed, this inactivation gate can be latched shut by a metal ion that bridges cysteines introduced at the outer mouth in each of the four subunits<sup>35,36</sup>. This inactivation process (normally slower than N-type inactivation) probably has a function in regulating repetitive electrical activity; its sensitivity to  $[K^+]$  may also determine a physiological response to accumulation

of extracellular  $K^+$  (refs 37, 38).

The structural details of C-type inactivation probably resemble the deformation of the KcsA selectivity filter that is seen<sup>4</sup> when those channels are crystallized with very low  $[K^+]$ : the selectivity filter contains fewer  $K^+$  ions, and instead of pointing towards the central axis, the carbonyl oxygens of the filter project obliquely, with a partial collapse of the filter. In some voltage-gated  $K^+$  channels, the inactivated selectivity filter can continue to conduct  $Na^+$  ions when all  $K^+$  is removed, suggesting a slightly different collapsed form where the carbonyl oxygens can now comfortably accommodate a  $Na^+$  ion<sup>39</sup>.

Single channel measurements<sup>40,41</sup> in voltage-gated  $K^+$  channels have suggested that even during the normal activation process (which at least in Shaker involves the S6 gate<sup>14</sup>), there may be movements of the selectivity filter. But gating at the selectivity filter may have an even more prominent role in other relatives of the voltage-gated  $K^+$  channels. In CNG channels<sup>42</sup> (but not HCN channels<sup>43</sup>) the selectivity filter apparently acts as the principal gate of the channel: there is nearly free access from the intracellular solution to the S6 region even in the closed state of the channel, although there is some change in size restriction with gating<sup>42</sup>, and there are clear conformational changes in S6 (ref. 44).

Overall, it seems probable that the basic functioning of the S6 gate and the selectivity filter gate are conserved among different channels: the S6 gate moves in response to a transmembrane voltage sensor or intracellular sensor domain, and the selectivity filter may react to the change in S6 by opening or closing. The conserved glycine that acts as a gating hinge in the MthK channel probably helps to decouple these two motions, but not completely. Depending on the structural details, the S6 gate may close completely (as in the Shaker and HCN channels), or may remain ajar even in the ‘closed’ state (as in the CNG and small-conductance,  $Ca^{2+}$ -activated  $K^+$  (SK) channels). Also depending on the details, the selectivity filter gate may remain always open, may respond to S6 movement by opening or closing, or may respond directly to voltage sensor motions.

### Gating sensors for voltage and ligands

Control of these gating motions by voltage (or in the case of other family members, by ligand binding) is essential for the channels’ signalling function. Before considering control by voltage, I will discuss two sensor mechanisms that are better understood at the structural level. Both of these involve intracellular sensor domains that are directly attached to the C-terminal end of the S6 region (a motif common to many members of the family; Box 1).

The MthK channel—a bacterial 2TM channel already mentioned for its importance for understanding both permeation and gating—has recently given us a new insight into one possible sensor mechanism used by the tetrameric 6TM channels. Similar to other channels in the ligand-gated branch of the family (Box 1, lower right panel), the MthK channel has a C-terminal sensor domain. The RCK (regulator of  $K^+$  conductance) domain used here is found also in other  $K^+$  channels such as an *Escherichia coli* 6TM channel and in a mammalian high-conductance,  $Ca^{2+}$ -activated  $K^+$  (BK) channel<sup>45</sup>. The original finding that RCK domains form homodimers fit with the general impression that the four C-terminal sensor domains of a tetrameric channel might function as two dimers—a ‘dimer of dimers’ pattern<sup>46</sup>. But the MthK channel was a surprise: a functional channel contains eight RCK domains, one on each channel subunit and one made in a soluble form by initiation at an internal methionine of the bacterial gene<sup>47</sup>. A tight and invariant dimer interface connects each channel domain with a soluble domain, and these four dimers (each displayed as a single block in Fig. 3, top panel) then form a ring with four-fold symmetry. A second interface (between the neighbouring dimers) has a different appearance in the two known crystal forms of the RCK domains, suggesting a remarkable and

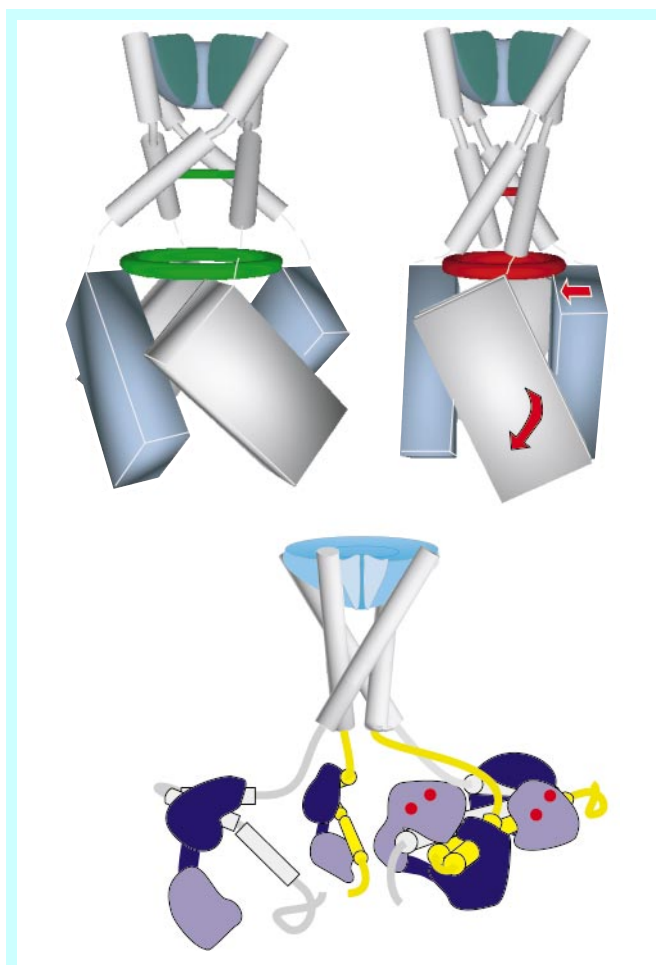


**Figure 3** Two sensor domains that govern gating in the  $K^+$  channel family. The top panel shows the proposed sensor-gating mechanism<sup>47</sup> for the calcium-gated MthK channel. Each rectangular box represents a dimer of two RCK domains (one attached to the channel subunit, one produced as a soluble protein). The open structure on the left has been observed for MthK with  $Ca^{2+}$  bound (although the linker between the channel domain and the sensor domain is not resolved). The closed structure on the right is proposed, on the basis of the closed channel structure of KcsA<sup>3</sup> and the related RCK domain from the *E. coli*  $K^+$  channel<sup>45</sup>. A change at the interface between neighbouring RCK dimers (which would be produced in MthK by  $Ca^{2+}$  dissociation) could close the channel by rotating the dimers and contracting the ‘gating ring’. The bottom panel shows the proposed sensor mechanism for the calcium-gated SK channel<sup>52</sup>. The two subunits on the left show  $Ca^{2+}$ -free and monomeric CaM (blue). The two subunits on the right show how binding of  $Ca^{2+}$  ions (red) to CaM (blue) produces dimerization of the post-S6 C-terminal tails (shown alternately in grey and yellow).

elegant transduction mechanism. By changing from one form of the secondary interface to another, the 'gating ring' could contract and expand, prying open the S6 gate of the attached channel domain (Fig. 3, top panel).

Other ligand-gated channels in the family are likely to use multimeric sensor domains. The CNG channels use a C-terminal nucleotide-binding domain that is closely related to the dimeric catabolite activator protein of bacteria<sup>48</sup>. The distantly related glutamate receptors—'upside down' K<sup>+</sup> channels with their transmembrane domains flipped and the ligand sensor on the extracellular side<sup>49</sup>—seem to have an important dimer relationship between their sensor domains<sup>50</sup>.

Structural evidence for a possible dimer-of-dimers sensor mechanism comes from another type of Ca<sup>2+</sup>-activated channel that appears to signal by Ca<sup>2+</sup>-induced association of sensors connected to the S6 region<sup>51,52</sup>. These 'SK' channels have a calmodulin-binding domain (CaMBD) located immediately adjacent to each S6; calmodulin (CaM) is stably bound here even in the absence of Ca<sup>2+</sup>. Studies of the detached CaM–CaMBD complex show that it behaves like a monomer in the absence of Ca<sup>2+</sup>, but dimerizes in the presence of Ca<sup>2+</sup>. The structure of this Ca<sup>2+</sup>-induced dimer shows an intimate reciprocal relationship between two CaM–CaMBD structures, with each CaM embracing both CaMBDs (Fig. 3, bottom). As in any dimer of dimers arrangement, formation of such dimers between neighbouring subunits would break the four-fold symmetry of the transmembrane channel; somehow this dimerization would produce a conformational change in the channel domain that opens the pore. Alternatively, with a modest change in the structure (and using the same protein interfaces seen in the crystal dimer structure), the four CaM–CaMBD complexes might form a four-fold symmetric tetramer upon Ca<sup>2+</sup> binding.

### The elusive voltage sensor

The voltage sensor is obviously central to the function of the voltage-gated K<sup>+</sup> channels, but its three-dimensional structure is still unknown. There is, however, a great deal of functional information about voltage sensing.

The transmembrane voltage must be sensed by a structure that moves charge at least partially across the membrane. The energetics of voltage gating, together with direct electrical measurements of the gating charge movement, show that as many as four charges per channel subunit are effectively translocated across the membrane as the channel switches between closed and open states<sup>53</sup>.

The expectation that transmembrane charges would be responsible for voltage sensing made it relatively easy to recognize the probable voltage sensor in the first channels cloned and sequenced<sup>54</sup>. The only sequence motif conserved across all voltage-gated ion channels (Na<sup>+</sup>, Ca<sup>2+</sup>, K<sup>+</sup>) is in the fourth transmembrane region (S4), which at every third position has a positively charged arginine or lysine residue. Mutations of these charges have complicated effects on voltage gating, but the ultimate interpretation of these experiments is that the S4 charges are indeed the critical gating charges<sup>55,56</sup>. These charges in the transmembrane region are energetically disfavoured (as discussed above for ion permeation); two possible mechanisms to compensate for this are negative countercharges in the S2 transmembrane region<sup>55,57</sup> and water-filled 'canals'<sup>58</sup> at each end of the S4 transmembrane region. The canals also focus the voltage drop across a thin septum, allowing a small physical movement to have large electrostatic consequences<sup>58</sup>.

Translocation of these S4 charges from one side of the membrane to the other can be confirmed biochemically, by replacing a charged residue with cysteine and applying cysteine modifying agents to one side or another<sup>59,60</sup>. A position accessible from the intracellular side at negative voltage can become accessible from the outside at positive voltage. Remarkably little of the S4 is actually buried in the membrane: when one charge position is accessible from the

outside, a site only six residues away in the sequence is accessible from the inside. This too is consistent with the idea of water-filled access pathways at each end.

Altogether, the four segments S1–S4 are presumed to form the voltage sensor domain. On the basis of the pattern of sequence conservation, cysteine accessibility, and tolerance for substitution, all are probably mainly  $\alpha$ -helical<sup>61–64</sup>. The pattern of the charged residues at every third position led to the early proposal of a 'helical screw' motion<sup>65,66</sup>: the S4 would advance screw-like to move each charge to the position of the next charge (or the next, and so on), thereby maintaining the charge distribution in the core while producing an overall translocation of charge across the membrane.

Many physical measurements have been made on fluorescence probes attached to cysteines placed in or near the S4, in an attempt to infer the motion of the voltage sensor. The pattern of fluorescence changes and the pattern of distances estimated from resonance energy transfer have roughly agreed with the idea of a rotation<sup>67,68</sup>. Yet all of the measured distance changes (particularly from the measurements with the highest precision) are very small (about 1 Å) and seem inconsistent with the popular proposal of a substantial rotation. There are many other ways in which the effective translocation of charge could be accomplished, such as the relative lateral movement of crossed helices or a rocking motion at the interface between two domains. Solving this particular puzzle would be greatly helped by some knowledge of the three-dimensional structure.

### The coupling problem

Unlike the ligand-binding domains attached directly to S6, the transmembrane voltage sensor does not have an obvious specific mechanism for coupling to the channel gates. Two possibilities have come to light recently. One is a direct coupling between the voltage sensor and the selectivity filter gate—in Shaker K<sup>+</sup> channels, activation gating produces a close approach between the extracellular part of the S4 and the region flanking the selectivity filter<sup>69</sup>. This then produces an allosteric effect on slow inactivation (involving the selectivity filter gate). At the intracellular side of the channel, a different site has been proposed<sup>70</sup> for coupling between S4 movement and the S6 activation gate: some sort of tight association between the S4–S5 linker and the intracellular projection of S6.

On the basis of the two best-known sensor mechanisms described in the previous section, it seems probable that a consistent theme of coupling will be that changes in quaternary structure of a sensor (such as ring expansion/contraction or domain multimerization) are transduced to the gating motions of the pore. It may therefore be tricky to identify a specific functional link between sensor and pore: the linkage may comprise a small number of 'tie-rods' with identifiable importance, or it may consist of an entire domain interface.

Dissecting these coupling mechanisms will of course be easier when we know the whole structure of a voltage-gated channel; however, particularly in this case, structure will not be enough, and careful mutagenesis and functional measurements will probably be required too. The fascination of the coupling problem is enhanced when one remembers that certain channels (for example, the HCN channels) have opposite relationships between voltage sensor movement and S6 gating: it appears that the same S6 gate used by 'normal' voltage-gated K<sup>+</sup> channels closes at positive voltages rather than negative voltages<sup>43</sup> (although S4 has the normal positive charges and presumably the normal direction of motion).

### Outlook

A combination of functional probing of channel proteins and recent structural advances have given clear pictures for many of the essential functions of the voltage-gated K<sup>+</sup> channels and their relatives. The remarkable optimizations of these channels for permitting rapid and selective ion flow across the hostile barrier

of the cell membrane are now mostly apparent, as is the basic repertoire of conformational changes used to gate this flow. We now see the outlines of two general approaches used by intracellular sensor domains to manipulate the channel gates, and some tantalizing details of the transmembrane voltage sensor itself. Many challenges remain in learning how the intricate machinery is integrated into a functional whole, and into the larger function of cellular signalling. □

doi:10.1038/nature00978.

1. Hodgkin, A. L. & Huxley, A. F. A quantitative description of membrane current and its application to conduction and excitation in nerve. *J. Physiol. (Lond.)* **117**, 500–544 (1952).
2. Latorre, R. & Miller, C. Conduction and selectivity in potassium channels. *J. Membr. Biol.* **71**, 11–30 (1983).
3. Doyle, D. A. *et al.* The structure of the potassium channel: molecular basis of potassium conduction and selectivity. *Science* **280**, 69–77 (1998).
4. Zhou, Y., Morais Cabral, J. H., Kaufman, A. & MacKinnon, R. Chemistry of ion hydration and coordination revealed by a K<sup>+</sup> channel-Fab complex at 2.0 Å resolution. *Nature* **414**, 43–48 (2001).
5. Morais-Cabral, J. H., Zhou, Y. & MacKinnon, R. Energetic optimization of ion conduction rate by the K<sup>+</sup> selectivity filter. *Nature* **414**, 37–42 (2001).
6. Jiang, Y. *et al.* The open pore conformation of potassium channels. *Nature* **417**, 523–526 (2002).
7. Roux, B. & MacKinnon, R. The cavity and pore helices in the KcsA K<sup>+</sup> channel: electrostatic stabilization of monovalent cations. *Science* **285**, 100–102 (1999).
8. Dutzler, R., Campbell, E. B., Cadene, M., Chait, B. T. & MacKinnon, R. X-ray structure of a CIC chloride channel at 3.0 Å reveals the molecular basis of anion selectivity. *Nature* **415**, 287–294 (2002).
9. Armstrong, C. M. Ionic pores, gates, and gating currents. *Q. Rev. Biophys.* **7**, 179–210 (1975).
10. Hodgkin, A. L. & Keynes, R. D. The potassium permeability of a giant nerve fibre. *J. Physiol. (Lond.)* **128**, 61–88 (1955).
11. Hille, B. & Schwarz, W. Potassium channels as multi-ion single-file pores. *J. Gen. Physiol.* **72**, 409–442 (1978).
12. Spassova, M. & Lu, Z. Coupled ion movement underlies rectification in an inward-rectifier K<sup>+</sup> channel. *J. Gen. Physiol.* **112**, 211–221 (1998).
13. Liu, Y., Holmgren, M., Jurman, M. E. & Yellen, G. Gated access to the pore of a voltage-dependent K<sup>+</sup> channel. *Neuron* **19**, 175–184 (1997).
14. del Camino, D. & Yellen, G. Tight steric closure at the intracellular activation gate of a voltage-gated K<sup>+</sup> channel. *Neuron* **32**, 649–656 (2001).
15. del Camino, D., Holmgren, M., Liu, Y. & Yellen, G. Blocker protection in the pore of a voltage-gated K<sup>+</sup> channel and its structural implications. *Nature* **403**, 321–325 (2000).
16. Holmgren, M., Shin, K. S. & Yellen, G. The activation gate of a voltage-gated K<sup>+</sup> channel can be trapped in the open state by an intersubunit metal bridge. *Neuron* **21**, 617–621 (1998).
17. Perozo, E., Cortes, D. M. & Cuello, L. G. Structural rearrangements underlying K<sup>+</sup>-channel activation gating. *Science* **285**, 73–78 (1999).
18. Armstrong, C. M. Interaction of tetraethylammonium ion derivatives with the potassium channels of giant axon. *J. Gen. Physiol.* **58**, 413–437 (1971).
19. Holmgren, M., Smith, P. L. & Yellen, G. Trapping of organic blockers by closing of voltage-dependent K<sup>+</sup> channels: evidence for a trap door mechanism of activation gating. *J. Gen. Physiol.* **109**, 527–535 (1997).
20. Hoshi, T., Zagotta, W. N. & Aldrich, R. W. Biophysical and molecular mechanisms of Shaker potassium channel inactivation. *Science* **250**, 533–538 (1990).
21. Rettig, J. *et al.* Inactivation properties of voltage-gated K<sup>+</sup> channels altered by presence of β-subunit. *Nature* **369**, 289–294 (1994).
22. Zagotta, W. N., Hoshi, T. & Aldrich, R. W. Restoration of inactivation in mutants of Shaker K<sup>+</sup> channels by a peptide derived from ShB. *Science* **250**, 568–571 (1990).
23. Murrell-Lagnado, R. D. & Aldrich, R. W. Interactions of amino terminal domains of Shaker K channels with a pore blocking site studied with synthetic peptides. *J. Gen. Physiol.* **102**, 949–975 (1993).
24. Murrell-Lagnado, R. D. & Aldrich, R. W. Energetics of Shaker K channels block by inactivation peptides. *J. Gen. Physiol.* **102**, 977–1003 (1993).
25. Choi, K. L., Aldrich, R. W. & Yellen, G. Tetraethylammonium blockade distinguishes two inactivation mechanisms in voltage-activated K<sup>+</sup> channels. *Proc. Natl Acad. Sci. USA* **88**, 5092–5095 (1991).
26. Demo, S. D. & Yellen, G. The inactivation gate of the Shaker K<sup>+</sup> channel behaves like an open-channel blocker. *Neuron* **7**, 743–753 (1991).
27. Zhou, M., Morais-Cabral, J. H., Mann, S. & MacKinnon, R. Potassium channel receptor site for the inactivation gate and quaternary amine inhibitors. *Nature* **411**, 657–661 (2001).
28. Ruppersberg, J. P. *et al.* Regulation of fast inactivation of cloned mammalian I<sub>K(A)</sub> channels by cysteine oxidation. *Nature* **352**, 711–714 (1991).
29. Roeper, J. *et al.* NIP domain prevents N-type inactivation in voltage-gated potassium channels. *Nature* **391**, 390–393 (1998).
30. Gulbis, J. M., Mann, S. & MacKinnon, R. Structure of a voltage-dependent K<sup>+</sup> channel beta subunit. *Cell* **97**, 943–952 (1999).
31. Kobertz, W. R., Williams, C. & Miller, C. Hanging gondola structure of the T1 domain in a voltage-gated K<sup>+</sup> channel. *Biochemistry* **39**, 10347–10352 (2000).
32. Sokolova, O., Kolmakova-Partensky, L. & Grigorieff, N. Three-dimensional structure of a voltage-gated potassium channel at 2.5 nm resolution. *Structure (Camb.)* **9**, 215–220 (2001).
33. Hoshi, T., Zagotta, W. N. & Aldrich, R. W. Two types of inactivation in Shaker K<sup>+</sup> channels: effects of alterations in the carboxy-terminal region. *Neuron* **7**, 547–556 (1991).
34. López-Barneo, J., Hoshi, T., Heinemann, S. H. & Aldrich, R. W. Effects of external cations and mutations in the pore region on C-type inactivation of Shaker potassium channels. *Recept. Channels* **1**, 61–71 (1993).
35. Yellen, G., Sodickson, D., Chen, T.-Y. & Jurman, M. E. An engineered cysteine in the external mouth of a K<sup>+</sup> channel allows inactivation to be modulated by metal binding. *Biophys. J.* **66**, 1068–1075 (1994).
36. Liu, Y., Jurman, M. E. & Yellen, G. Dynamic rearrangement of the outer mouth of a K<sup>+</sup> channel during gating. *Neuron* **16**, 859–867 (1996).
37. Pardo, L. A. *et al.* Extracellular K<sup>+</sup> specifically modulates a rat brain K<sup>+</sup> channel. *Proc. Natl Acad. Sci. USA* **89**, 2466–2470 (1992).
38. Baukrowitz, T. & Yellen, G. Modulation of K<sup>+</sup> current by frequency and external [K<sup>+</sup>]: a tale of two inactivation mechanisms. *Neuron* **15**, 951–960 (1995).
39. Kiss, L., LoTurco, J. & Korn, S. J. Contribution of the selectivity filter to inactivation in potassium channels. *Biophys. J.* **76**, 253–263 (1999).
40. Chapman, M. L., VanDongen, H. M. & VanDongen, A. M. Activation-dependent subconductance levels in the drk1 K<sup>+</sup> channel suggest a subunit basis for ion permeation and gating. *Biophys. J.* **72**, 708–719 (1997).
41. Zheng, J. & Sigworth, F. J. Selectivity changes during activation of mutant Shaker potassium channels. *J. Gen. Physiol.* **110**, 101–117 (1997).
42. Flynn, G. E. & Zagotta, W. N. Conformational changes in S6 coupled to the opening of cyclic nucleotide-gated channels. *Neuron* **30**, 689–698 (2001).
43. Rothberg, B. S., Shin, K. S., Phale, P. S. & Yellen, G. Voltage-controlled gating at the intracellular entrance to a hyperpolarization-activated cation channel. *J. Gen. Physiol.* **119**, 83–91 (2002).
44. Johnson, J. P. Jr & Zagotta, W. N. Rotational movement during cyclic nucleotide-gated channel opening. *Nature* **412**, 917–921 (2001).
45. Jiang, Y., Pico, A., Cadene, M., Chait, B. T. & MacKinnon, R. Structure of the RCK domain from the *E. coli* K<sup>+</sup> channel and demonstration of its presence in the human BK channel. *Neuron* **29**, 593–601 (2001).
46. Liu, D. T., Tibbs, G. R., Paoletti, P. & Siegelbaum, S. A. Constraining ligand-binding site stoichiometry suggests that a cyclic nucleotide-gated channel is composed of two functional dimers. *Neuron* **21**, 235–248 (1998).
47. Jiang, Y. *et al.* Crystal structure and mechanism of a calcium-gated potassium channel. *Nature* **417**, 515–522 (2002).
48. Weber, I. T. & Steitz, T. A. Structure of a complex of catabolite gene activator protein and cyclic AMP refined at 2.5 Å resolution. *J. Mol. Biol.* **198**, 311–326 (1987).
49. Chen, G. Q., Cui, C., Mayer, M. L. & Gouaux, E. Functional characterization of a potassium-selective prokaryotic glutamate receptor. *Nature* **402**, 817–821 (1999).
50. Sun, Y. *et al.* Mechanism of glutamate receptor desensitization. *Nature* **417**, 245–253 (2002).
51. Xia, X. M. *et al.* Mechanism of calcium gating in small-conductance calcium-activated potassium channels. *Nature* **395**, 503–507 (1998).
52. Schumacher, M. A., Rivard, A. F., Bachinger, H. P. & Adelman, J. P. Structure of the gating domain of a Ca<sup>2+</sup>-activated K<sup>+</sup> channel complexed with Ca<sup>2+</sup>/calmodulin. *Nature* **410**, 1120–1124 (2001).
53. Sigworth, F. J. Voltage gating of ion channels. *Q. Rev. Biophys.* **27**, 1–40 (1994).
54. Noda, M. *et al.* Primary structure of *Electrophorus electricus* sodium channel deduced from cDNA sequence. *Nature* **312**, 121–127 (1984).
55. Seoh, S. A., Sigg, D., Papazian, D. M. & Bezanilla, F. Voltage-sensing residues in the S2 and S4 segments of the Shaker K<sup>+</sup> channel. *Neuron* **16**, 1159–1167 (1996).
56. Aggarwal, S. K. & MacKinnon, R. Contribution of the S4 segment to gating charge in the Shaker K<sup>+</sup> channel. *Neuron* **16**, 1169–1177 (1996).
57. Tiwari-Woodruff, S. K., Lin, M. A., Schulteis, C. T. & Papazian, D. M. Voltage-dependent structural interactions in the Shaker K<sup>+</sup> channel. *J. Gen. Physiol.* **115**, 123–138 (2000).
58. Islas, L. D. & Sigworth, F. J. Electrostatics and the gating pore of Shaker potassium channels. *J. Gen. Physiol.* **117**, 69–89 (2001).
59. Yang, N., George, A. L. Jr & Horn, R. Molecular basis of charge movement in voltage-gated sodium channels. *Neuron* **16**, 113–122 (1996).
60. Larsson, H. P., Baker, O. S., Dhillon, D. S. & Isacoff, E. Y. Transmembrane movement of the Shaker K<sup>+</sup> channel S4. *Neuron* **16**, 387–397 (1996).
61. Durell, S. R., Hao, Y. & Guy, H. R. Structural models of the transmembrane region of voltage-gated and other K<sup>+</sup> channels in open, closed, and inactivated conformations. *J. Struct. Biol.* **121**, 263–284 (1998).
62. Monks, S. A., Needleman, D. J. & Miller, C. Helical structure and packing orientation of the S2 segment in the Shaker K<sup>+</sup> channel. *J. Gen. Physiol.* **113**, 415–423 (1999).
63. Li-Smerin, Y., Hackos, D. H. & Swartz, K. J. alpha-helical structural elements within the voltage-sensing domains of a K<sup>+</sup> channel. *J. Gen. Physiol.* **115**, 33–50 (2000).
64. Hong, K. H. & Miller, C. The lipid-protein interface of a Shaker K<sup>+</sup> channel. *J. Gen. Physiol.* **115**, 51–58 (2000).
65. Guy, H. R. & Seetharamulu, P. Molecular model of the action potential sodium channel. *Proc. Natl Acad. Sci. USA* **83**, 508–512 (1986).
66. Catterall, W. A. Voltage-dependent gating of sodium channels: correlating structure and function. *Trends Neurosci.* **9**, 7–10 (1986).
67. Glauner, K. S., Mannuzzu, L. M., Gandhi, C. S. & Isacoff, E. Y. Spectroscopic mapping of voltage sensor movement in the Shaker potassium channel. *Nature* **402**, 813–817 (1999).
68. Cha, A., Snyder, G. E., Selvin, P. R. & Bezanilla, F. Atomic scale movement of the voltage-sensing region in a potassium channel measured via spectroscopy. *Nature* **402**, 809–813 (1999).
69. Elinder, F., Mannikko, R. & Larsson, H. P. S4 charges move close to residues in the pore domain during activation in a K channel. *J. Gen. Physiol.* **118**, 1–10 (2001).
70. Tristani-Firouzi, M., Chen, J. & Sanguinetti, M. C. Interactions between S4-S5 linker and S6 transmembrane domain modulate gating of HERG K<sup>+</sup> channels. *J. Biol. Chem.* **277**, 18994–19000 (2002).
71. Heginbotham, L., Abramson, T. & MacKinnon, R. A functional connection between the pores of distantly related ion channels as revealed by mutant K<sup>+</sup> channels. *Science* **258**, 1152–1155 (1992).
72. Ren, D. *et al.* A prokaryotic voltage-gated sodium channel. *Science* **294**, 2372–2375 (2001).
73. Kreuzsch, A., Pfaffinger, P. J., Stevens, C. F. & Choe, S. Crystal structure of the tetramerization domain of the Shaker potassium channel. *Nature* **392**, 945–948 (1998).
74. Gulbis, J. M., Zhou, M., Mann, S. & MacKinnon, R. Structure of the cytoplasmic beta subunit-T1 assembly of voltage-dependent K<sup>+</sup> channels. *Science* **289**, 123–127 (2000).
75. Shen, N. V. & Pfaffinger, P. J. Molecular recognition and assembly sequences involved in the subfamily-specific assembly of voltage-gated K<sup>+</sup> channel subunit proteins. *Neuron* **14**, 625–633 (1995).

76. Holmes, T. C., Fadool, D. A., Ren, R. & Levitan, I. B. Association of Src tyrosine kinase with a human potassium channel mediated by SH3 domain. *Science* **274**, 2089–2091 (1996).
77. Doyle, D. A. *et al.* Crystal structures of a complexed and peptide-free membrane protein-binding domain: molecular basis of peptide recognition by PDZ. *Cell* **85**, 1067–1076 (1996).
78. Wallner, M., Meera, P. & Toro, L. Determinant for  $\beta$ -subunit regulation in high-conductance voltage-activated and  $\text{Ca}^{2+}$ -sensitive  $\text{K}^+$  channels: an additional transmembrane region at the N terminus. *Proc. Natl Acad. Sci. USA* **93**, 14922–14927 (1996).
79. Morais, C. J. *et al.* Crystal structure and functional analysis of the HERG potassium channel N terminus: a eukaryotic PAS domain. *Cell* **95**, 649–655 (1998).
80. Knaus, H. G., Eberhart, A., Kaczorowski, G. J. & Garcia, M. L. Covalent attachment of charybdotoxin to the  $\beta$ -subunit of the high conductance  $\text{Ca}^{2+}$ -activated  $\text{K}^+$  channel. Identification of the site of incorporation and implications for channel topology. *J. Biol. Chem.* **269**, 23336–23341 (1994).
81. Tapper, A. R. & George, A. L. Jr Location and orientation of minK within the I(Ks) potassium channel complex. *J. Biol. Chem.* **276**, 38249–38254 (2001).

## Acknowledgements

I would like to thank members of my laboratory and B. Bean for many discussions and for suggestions about the manuscript, and R. MacKinnon for advice about timing. My research was supported by the National Institutes of Health.

Correspondence and requests for materials should be addressed to the author (e-mail: gary\_yellen@hms.harvard.edu).